

**TITLE:** ARCHITECTURE AND DYNAMICS OF ISOTOPICALLY LABELLED  
MACROMOLECULES BY NUCLEAR MAGNETIC RESONANCE SPECTROSCOPY

**AUTHOR(S):** N. A. Matwiyoff

**SUBMITTED TO:** PROCEEDINGS -  
NATO A.S.I. Series on ESR and NMR of Paramagnetic Species  
in Biological and Related Systems.

**MASTER**

University of California

By acceptance of this article, the publisher recognizes that the U.S. Government retains a nonexclusive, royalty-free license to publish or reproduce the published form of this contribution, or to allow others to do so, for U.S. Government purposes.

The Los Alamos Scientific Laboratory requests that the publisher identify this article as work performed under the auspices of the U.S. Department of Energy.

**NOTICE**  
This report was prepared in an account of work sponsored by the United States Government. Neither the United States nor the United States Department of Energy, nor any of their employees, nor any of their contractors, subcontractors, or their employees, makes any warranty, express or implied, or assumes any legal liability or responsibility for the accuracy, completeness or usefulness of any information, apparatus, product or process disclosed, or represents that its use would not infringe privately owned rights.

**DISTRIBUTION OF THIS DOCUMENT IS UNLIMITED**



**LOS ALAMOS SCIENTIFIC LABORATORY**

Post Office Box 1663 Los Alamos, New Mexico 87545

An Affirmative Action/Equal Opportunity Employer

## ARCHITECTURE AND DYNAMICS OF ISOTOPICALLY LABELLED MACROMOLECULES BY NUCLEAR MAGNETIC RESONANCE SPECTROSCOPY\*

N. A. Matwiyoff

Los Alamos Scientific Laboratory  
University of California  
Los Alamos, New Mexico 87545 U.S.A.

### INTRODUCTION

The last two decades were a period of luxuriant growth in the X-Ray Crystallography of biological macromolecules that has led to remarkably detailed correlations between their structure and function (1). A particularly outstanding example is the elegant work of Perutz and his colleagues on the structure of hemoglobins which resemble "molecular lungs" (2) in their mode of O<sub>2</sub>/CO<sub>2</sub> binding and release. The family of serine proteases provide another example and, in this case, x-ray structural studies have resulted in an elaborate picture of the mechanism of the action of this class of enzymes (3,4); however, the detailed picture is not without its controversial elements (5).

As valuable as the x-ray structure of a biological macromolecule is, the picture it provides is a static one (6) of a molecule whose states of hydration and intermolecular association are much different than those under physiological conditions. The use of NMR spectroscopy in the study of biological molecules and macromolecular assemblages has grown even more dramatically than x-ray methods and, in part, this is because NMR provides a dynamic, conformationally averaged, picture of a molecule in solution that is complementary to the crystallographic "still photo". The resolution of the dynamic features of the structure by NMR, of course, is accomplished at the expense of specificity in the location of the atoms. An additional complication in NMR studies of proteins, for example, is that the large number of atoms generally prevents resolution of a single resonance for each nucleus and its assignment to a specific amino acid residue.

Of course, as discussed at length in these proceedings, intrinsic and extrinsic paramagnetic shift and relaxation reagents offer great promise in recovering the spatial specificity and in improving the resolution of the NMR experiments. An alternate method for accomplishing these latter objectives without perturbing the experimental system with extrinsic reagents, is to use NMR to monitor a protein specifically labeled with  $^{13}\text{C}$  or  $^{15}\text{N}$  enriched amino acids. An ancillary benefit is that specific labeling frequently allows an NMR study of the macromolecule in intact cells and tissues. This method is the subject for discussion in this paper which is not a comprehensive treatment but an illustrative survey of what appear to be the most promising areas for future development in the study of the architecture and dynamics of macromolecules and macromolecular assemblages, especially those containing proteins. To illustrate the full power of the technique at the outset, we will first briefly consider the  $^{13}\text{C}$  NMR spectra of cell suspensions specifically labeled with  $^{13}\text{C}$ .

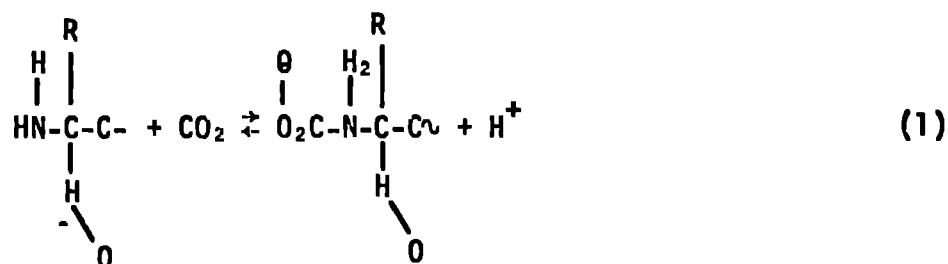
#### RED BLOOD CELL SUSPENSIONS

As we all know, the role of the red blood cell in physiological gas exchange is not only to deliver  $\text{O}_2$  from the lung to peripheral tissues but also to transport  $\text{CO}_2$ , the end product of respiration, to the lung. Although the mechanism of the uptake transport, and delivery of  $\text{O}_2$  by hemoglobin within the red blood cell is reasonably well understood (2), only in the past few years has the complexity of the physiological transport mechanism for  $\text{CO}_2$  begun to be unraveled. As we have learned more about  $\text{CO}_2$  transport, we have also come to appreciate that the physiological importance of  $\text{CO}_2$  may reside not only in its role of mediating pH and ionic strength but also in the regulation of enzyme activity through formation of carbamino complexes. As outlined in the following, the  $^{13}\text{C}$  NMR of  $^{13}\text{C}$  labeled systems has played a central role in the development of this understanding.

Matwiyoff and Needham (9) were the first to study the interaction between  $\text{CO}_2$  and hemoglobin in the red blood cell by  $^{13}\text{C}$  NMR techniques. A summary of their results is contained in Figure 1 and illustrates the  $^{13}\text{C}$  NMR spectra of packed human red blood cells in isotonic saline treated with [ $^{13}\text{C}$  (90 atom %)]  $\text{CO}_2$ . The resonances identified as a, b, and c (Figure 1b) did not occur in the spectra of red blood cells treated with natural  $^{13}\text{C}$  abundance  $\text{CO}_2$  and, on the basis of chemical shifts alone, resonances b and c, could be assigned to  $\text{HCO}_3^-$  ion and dissolved  $\text{CO}_2$ , respectively. The assignments were confirmed, however, by the addition of carbonic anhydrase which catalyzes the interchange between  $\text{CO}_2$  and the  $\text{HCO}_3^-$  ion, large concentrations of the enzyme leading to chemical exchange broadening (Figure 1c), and

eventual collapse of signals b and c to an exchange narrowed peak at the center of gravity of the original resonances. Signal a was not affected by the carbonic anhydrase treatment.

A clue to the origin of signal a was the early suggestion by Rossi-Bernardi and Roughton (10,11,12) that a significant fraction of the physiological CO<sub>2</sub> transport was in the form of carbamino complexes (structure shown in Figure 1) of the N-terminal valine residues of the hemoglobin chains, a suggestion supported by later studies of Kilmartin and Rossi-Bernardi (13,14,15) who showed that when the terminal α-amino groups of isolated hemoglobin were blocked by cyanate carbonylation, the O<sub>2</sub>-linked CO<sub>2</sub> interactions were reduced or obliterated. A confirmation that a was a resonance from a carbamino compound in the red blood cell system was obtained by <sup>13</sup>C NMR studies of carbamino derivatives of the common amino acids. Subsequently, Arnone (16) studied the x-ray structure of human deoxyhemoglobin crystals soaked in CO<sub>2</sub>/bicarbonate buffer (pH 7.4 and p<sub>CO<sub>2</sub></sub> = 1 atm) and showed that CO<sub>2</sub> does indeed form carbamino complexes with the valine N-terminal amino groups of the hemoglobin β chains. In more recent work, Gurd and co-workers (17,18) have studied, by <sup>13</sup>C NMR techniques, adduct formation of CO<sub>2</sub> with isolated hemoglobins and peptide hormones with the view of elucidating potential regulatory influences of carbamino formation. Because carbamino formation (equation 1) results in the introduction of a charged bulky group on the terminal amino function, one might expect in the general case that regulatory influences could be exerted through the formation of salt bridges and/or changes in the population of rotamers about the N-C bond. In the case of



deoxyhemoglobin itself, Arnone's x-ray studies (16) indicate that CO<sub>2</sub> binding to the terminal valine residues of the β chains merely displaces an ion from an anion binding site and does not produce any marked changes in the conformation of the deoxy β subunits. However, allosterically effective conformational changes may be too small to detect with x-ray methods and, in this context, it is interesting to note that <sup>13</sup>C NMR studies have shown (17) that the reduction of carbamino adduct formation accompanying the conversion of deoxy- to oxy-hemoglobin occurs predominantly at the terminal valines of the β subunits. Given the ubiquitousness of CO<sub>2</sub> and HCO<sub>3</sub><sup>-</sup> ion in biological systems, it

is likely, as Gurd has pointed out, that carbamino adducts may play a role in modifying the activities of enzymes with terminal amino groups having pK's near 7. Indeed, it has been shown that even the peptide hormones, angiotensin and bradykinin, form significant quantities of carbamino adducts at physiological pH and  $P_{CO_2}$  (18).

In a related context, there is another interesting feature of the spectra in Figure 1 -- spectrum C is for hemolyzed blood and one notes a pronounced broadening of the  $HCO_3^-$  and  $CO_2$  resonances compared to the whole blood spectrum. The red blood cell contains a high concentration of carbonic anhydrase ( $\sim 2$  mg) which may be loosely or tightly bound to the membrane. Hemolysis releases it, allowing it to more effectively catalyze the  $^{13}CO_2$  and  $H^{13}CO_3^-$  exchange which broadens both resonances. The apparent difference in the activity of the enzyme in whole and hemolyzed blood, which we do not understand as yet (but see 19) and which may suggest a function for carbonic anhydrase in the cell other than  $CO_2$  turnover, points to the importance of studying whole cell systems where possible.

Whereas the apparent decrease in the activity of the red blood cell carbonic anhydrase may be unusual, I would stress that the carbamino chemistry we are monitoring by looking through the cell with  $^{13}C$  NMR is completely normal. That is, hemoglobin carbamino formation conforms to the laws of mass action, rising with  $CO_2$  pressure and decreasing with decreasing pH in the red blood cell just as it does in homogeneous aqueous solutions as studied extensively by Gurd and co-workers at Indiana University (17,18). This is not too surprising -- physical chemistry is physical chemistry. It is stressed here because there is a folklore or mystique about the properties of the interior fluids of the cell which might lead to unusual chemistry - regions of high ionic strength, high viscosity, abnormal pH, polywater structure, etc. And, of course, it is difficult to get a fix on the properties of the interior of the cell without using a technique that violates its integrity. NMR provides a limited opportunity to probe the environment of intracellular constituent without perturbing the system. One well-known method based on NMR is to probe the intracellular pH by studying the pH dependent chemical shifts of intracellular phosphate derivatives. A less well known, though equally promising, NMR method for probing the intracellular environment is the study of intracellular viscosity by measuring the spin lattice relaxation and rotational correlation times of  $^{13}C$  labeled soluble intracellular constituents (21,22). Unfortunately time does not permit elaboration of these investigations but it could be noted that NMR studies have revealed nothing "abnormal" about the pH or viscosities of the intracellular fluids studied to date.

## STRUCTURAL CONSTITUENTS OF CELLS

In the preceding, we have outlined briefly a general kind of NMR approach to the analysis, chemical transformations, and environment of specific, isotopically labeled intracellular constituents. In principle, it is possible also to isotopically label individual structural components of the cells themselves. This is a promising area of investigation as well and one which has attracted a great deal of interest recently. Most attention has been devoted to the lipids of the cell membrane, both because of the ease with which they are labeled and their importance in cellular function. The cell membrane lipids, exemplified by the phospholipids depicted in Figure 2, have been judged on the basis of a number of physical studies (23) to be arranged in a bilayer structure and to be involved in a variety of cellular processes, including the maintenance of the cell permeability barrier and association with proteins to form functional entities. With regard to these functions, one parameter which appears critical is the mobility or fluidity of the lipid bilayer which, in turn, depends on the stiffness of the hydrocarbon chains and the way they are packed in the bilayer. This question has been studied in some detail by the use of  $^{13}\text{C}$  and  $^2\text{H}$  labeled fatty acids incorporated into natural and artificial membranes; and the nuclear spin lattice relaxation times of the hydrocarbon chains are not inconsistent with chain flexibilities and more classical measures of membrane permeabilities and transition temperatures for the transformation from the "solid" to "liquid crystalline" phases. These questions have been reviewed previously (24) and will not be considered at length here. Instead, we focus on the illustrative aspects of a unique  $^{13}\text{C}$  labeling experiment which has yielded valuable information about both the structural and dynamic properties of the polar phosphoryl, choline head groups of phospho lipids in natural and artificial membranes.

A central question about the disposition of membrane polar head groups, which is reciprocal to that asked about hydrocarbon residues, is whether these polar groups which interface with the aqueous phases at the extracellular or intracellular boundary are close packed or loose structures? Specifically, do the polar  $-\text{N}(\text{CH}_3)_3^+$  groups: (a) form rigid salt bridges with an adjacent charged phosphate group making a compact structure; or (b) interact strongly with the aqueous phase forming an extended mobile structure characterized by rotational freedom favored by the loose, and dynamic, water structure. We have studied this question by biosynthetically incorporating  $^{13}\text{C}$ -labeled choline (22,25) into Chinese Hamster Ovary (CHO) cells and studying the  $^{13}\text{C}$  spin lattice relaxation times and linewidths. Two types of labeling experiments were done: (1) the label was inserted into the N-methyl group alone; and (2) the label was inserted separately

into the N-CH<sub>3</sub> group, the 1-<sup>13</sup>C and the 2-<sup>13</sup>C positions and a mixture (1:3:3) was incorporated into the polar head group (the mixture was used rather than a uniformly labeled choline to avoid the complications of <sup>13</sup>C-<sup>13</sup>C coupling).

The [<sup>13</sup>C]choline N-trimethyl resonances exhibited by an aqueous suspension of CHO cells grown in a medium containing [<sup>13</sup>C-methyl]choline is reproduced in Figure 3. The line is narrow (14.8 Hz half-width at 21°C) and the T<sub>1</sub> was determined to be 400 ms at 21°C. Both observations show that the relaxation of the [<sup>13</sup>C]choline methyl groups in the CHO cells are determined by the internal motion of the choline methyl carbons. This was confirmed by showing that the relaxation time increased with increasing temperature; and exhibited an apparent activation energy of 4.3 kcal/mole, a value expected for a neopentyl-like barrier for the motion. The relaxation data could be fit with the model shown in Figure 4 in which motion of C-1 is restricted, whereas motion by R<sub>3</sub>, R<sub>2</sub>, and R<sub>1</sub> occur to a significant extent ( $\tau \approx 3.1 \times 10^{-11}$  s). Although a more appropriate model should incorporate a motional gradient R<sub>1</sub> > R<sub>2</sub> > R<sub>3</sub>, the point is established that the polar head groups do not adopt a compact structure but rather have significant freedom of motions which, in the aggregate, are isotropic enough that the <sup>13</sup>C line is narrow.

The spectra of the [1-<sup>13</sup>C], [2-<sup>13</sup>C], and [methyl-<sup>13</sup>C] labeled choline in CHO cell suspensions and in suspensions of vesicles prepared from the CHO cell lipids are even more interesting (Figure 5). In the spectrum obtained under conditions of simultaneous <sup>14</sup>N and <sup>1</sup>H (<sup>13</sup>C{<sup>14</sup>N, <sup>1</sup>H}) decoupling, the two and three bond <sup>31</sup>P-<sup>13</sup>C scalar coupling is evident as it is in the synthetic vesicle. The rationale behind using <sup>14</sup>N decoupling, though an interesting story in itself, need not concern us here. The interesting point is that the value of the three bond coupling constant allows an estimation of the conformation about the C-1-O bond from the expression derived by Smith and co-workers (26)

$$^3J_{CCOP} = 9.5 \cos^2\theta - 0.6 \theta$$

Trans coupling constants predicted from this equation are similar to those measured recently for cyclic sugar phosphates locked into a trans configuration (27). Analysis of the C-2-P coupling constants using this expression, together with the assumption that there is a rapid gauche  $\rightleftharpoons$  trans equilibrium leads to fractional trans probabilities of 61%, 64%, 65%, and 75% for dioleoyl, dipalmitoyl, and egg yolk lecithins, and the CHO cells, respectively.

It is clear that isotopic labeling in conjunction with NMR spectroscopy can provide valuable information about intact

cellular systems but it is well to point out that the field is still in its infancy and, because of the complexity of the systems involved, we can only expect partial answers to the simplest questions. We are usually talking about a heterogeneous population of cells and we have a variety of membrane systems which have an intrinsic asymmetry, a diverse population of structural and functional proteins distributed among membranes, ribosomes, chromatin, the cytosol, etc. The sheer complexity of the system has led some investigators to approach the problem from the other extreme -- label individual proteins, lipids, nucleic acids, etc.; study them individually; and then as part of a reconstituted macroscopic assemblage. This approach is likely to pay big dividends, even if only for the study of the individual macromolecules as an adjunct to x-ray crystallography. In the next section I would like to illustrate the approach with a labeled enzyme we have been studying.

#### $^{13}\text{C}$ LABELED ENZYMES: DIHYDROFOLATE REDUCTASE

Several recent studies of enzymes (5, 28-32) and proteins (21,33,34) have shown that the incorporation of  $^{13}\text{C}$  labeled amino acids into macromolecules can provide an excellent, non-perturbing NMR probe by which protein-ligand interactions can be studied. In our own group at the national stable isotopes resource at the Los Alamos Scientific Laboratory we have, in cooperation with Professor R. L. Blakley of the University of Iowa Medical School, initiated a series (35-38) of  $^{13}\text{C}$  NMR studies of the enzyme dihydrofolate reductase (DHFR) labeled with a number of  $^{13}\text{C}$  enriched amino acids. The enzyme catalyzes the NADPH-linked reduction of dihydrofolate to tetrahydrofolate which has an essential role in purine and pyrimidine biosynthesis. Apart from its convenient size (~20,000 daltons) for NMR studies, interest in the structure of the DHFR and its complexes derives from its clinical importance, the enzyme being the target of antineoplastic and antibacterial chemotherapeutic agents such as methotrexate and aminopterin. Although our studies are still in the early stages, the results which are surveyed in the following illustrate the potential and limitations of the method.

In Figure 6 are summarized the proton decoupled  $^{13}\text{C}$  NMR in the  $[\gamma\text{-}^{13}\text{C}]\text{-Trp}$  region for DHFR isolated from Streptococcus faecium grown in medium containing  $[\gamma\text{-}^{13}\text{C}]\text{tryptophan}$ . The enzyme S. faecium contains four tryptophan (Trp) residues at the following positions in the amino acid sequence (39): Trp-6; Trp-22; Trp-115; and Trp-160. In the crystal structure of the Lactobacillus casei enzyme complexes (40,41), Trp-5 and Trp-21 correspond to positions 6 and 22 of the S. faecium enzyme in highly conserved sequences and are buried in hydrophobic pockets in the ternary DHFR-MTX-NADPH complex. The two other residues of the Lactobacillus casei enzyme, Trp-133 and Trp-158, do not



occur in such highly conserved sequences; and the former is partially and the latter is fully accessible to solvent. Urea denaturation of the enzyme with consequent solvent exposure of all Trp residues causes collapse of the  $^{13}\text{C}$  spectrum to three closely spaced narrow lines at 109.5, 109.7, and 109.9 ppm (Figure 7). Thus, it is likely that the resonance at 110.4 ppm in the native enzyme (Figure 6) is either Trp-115 or Trp-160. Although a likely assignment for the other solvent exposed Trp is the double resonance at  $\sim 110$  ppm, the peak at 111 ppm is assigned to it for the reasons discussed below.

The resonance centered at  $\sim 110$  ppm and  $\sim 106$  ppm are more informative in structural terms. First, the former is a double peak with relative intensities of the components of 2:3. Since the separation of these peaks is 0.2 ppm at both 25.2 MHz and 90 MHz, the most reasonable interpretation of this double resonance is that it arises from the occupation of two distinct environments by a single Trp residue. It is probably Trp-6 which is deeply buried (41,42) in a hydrophobic pocket composed of phenylalanine, leucine, valine, methionine, etc. side chains. As described by London, *et al.* (37), the Trp probably samples these two environments by a slow, restricted rotation about the  $\text{C}_\beta\text{-C}_\gamma$  bond with some rotation about the  $\text{C}_\alpha\text{-C}_\beta$  bond as well. A slow rotation about these bonds would be expected from steric interactions of the bulky indole side chain in the compact, highly organized region of the DHFR structure occupied by Trp-6.

The remaining resonance at  $\sim 106$  ppm, which can be assigned by difference to Trp-22, exhibits some unusual features. First, the line is very broad for a quaternary resonance in an enzyme of this molecular weight (half-width of  $\sim 30$  Hz at  $25^\circ\text{C}$ ) and, second, the linewidth increases with increasing temperature, accompanied by an 0.8 ppm downfield shift of the resonance as the temperature increases from 5 to  $25^\circ\text{C}$ . These data are consistent with a slow exchange of the Trp-22 residue between two distinct chemical environments with unequal populations, the minor component (<10%) having an  $\sim 5$  ppm shift downfield of the major resonance at  $\sim 106$  ppm. Because of the small population of the former, its  $^{13}\text{C}$  resonance will be undetectable. The temperature dependence of the line shapes of the 106 ppm resonance are consistent with this interpretation, the lifetime of the major species being  $\sim 0.03$  s at  $15^\circ\text{C}$ .

The  $^{13}\text{C}$  spectra of DHFR as it gradually uncoils when titrated with urea (Figure 7) provide some insight into the nature of the chemical exchange process involving Trp-22. As the urea concentration increases, the spectra are consistent with a gradual depopulation of the site giving rise to the resonance at  $\sim 106$  ppm. This is accompanied by a broadening of the  $\sim 106$  ppm resonance and the apparent growth of a broader one in the region

of 110 ppm (note particularly the 3 M urea spectrum, Figure 7). It is generally accepted that urea denaturation of a protein results in a random coil configuration, exposing hydrophobically "buried" residues to the solvent. Although the structures of intermediate states on the route to denaturation are uncertain, it seems reasonable that these would correspond to progressively open structures associated with the gradual disruption of  $\beta$ -pleated sheets and  $\alpha$ -helices. This suggests to us that: the Trp-22 site characterized by the  $\sim 106$  ppm resonance is a pre-dominately hydrophobic one in which the unusual chemical shift is induced by electric field effects of nearby immobilized polar or charged groups; the site corresponding to the  $\sim 110$  ppm resonance is a solvent exposed one; and that Trp-22 samples these two environments by breathing motions of DHFR which may be localized to the region of the inner cavity surface where Trp-22 resides or may involve the conversion of the whole structure from one well-defined conformation to another.

Continuing in this vein, it is interesting to speculate on the structural basis of this chemical exchange process in terms of the discussion of the structure of DHFR complexes by D. A. Matthews (42). Trp-22 (Trp-21 in the Lactobacillus casei enzyme) resides on the inner surface of the large cavity in which MTX and the nicotinamide (NA) ring of NADPH are bound. In the DHFR-MTX-NADPH complex, the Trp-22 indole side chain is in Van der Waal's contact with the carboxamide portion of the NA ring and is in a hydrophobic pocket completely inaccessible to solvent. In the MTX or NADPH binary complexes, approximately three-quarters of the indole side chain is buried in the pocket with about one-quarter of the solid angle of the indole ring being exposed to solvent. Matthews (42) suggests that in the uncomplexed enzyme, the vacant, active site would permit solvent access to approximately half of the solid angle around the indole side chain of Trp-22. Thus, in the progression DHFR  $\rightarrow$  Binary Complex  $\rightarrow$  Ternary Complex, the Trp-22 residue becomes progressively more immobilized in a hydrophobic pocket. These structural considerations, broadly interpreted, are entirely consistent with the preceding discussion of the  $^{13}\text{C}$  spectra of the native and urea denatured proteins which are at the extreme structural disorganization at the surface of the active site cavity. The other extreme of structural organization is provided by the binary and ternary complexes, DHFR-NADPH, DHFR-MTX, and DHFR-NADPH-MTX, whose  $^{13}\text{C}$  spectra are summarized in Figure 8. As evident from the spectra, binding of NADPH in the binary complex narrows the Trp-22  $\sim 106$  ppm resonance somewhat compared to the uncomplexed enzyme whereas in the binary DHFR-MTX complex the corresponding resonance narrows sharply. As expected from Matthews' evaluation of the structures, the resonance in question is also narrow in the ternary DHFR-NADPH-MTX complex. In these systems, as well as in the urea treated enzyme, spectral changes occur also in the resonances assigned

to Trp-6 but these will not be considered in detail here. We note only that in the urea treated enzyme not only does the Trp-6 resonance broaden but also the population of the conformation corresponding to the downfield component of the resonance increases markedly.

Finally, with respect to the assignments we have made of the Trp  $C_\gamma$  resonances, the results of some preliminary nitroxide spin label studies with the analog of NADPH, are of interest (Figure 9). As evident from the spectra of DHFR containing the spin label NAPH-SL (43), the resonances assigned to Trp-115 and Trp-160 are unaffected by the paramagnetic center. This is not unexpected since these residues are more than 15 Å away from the expected location of the nitroxyl radical (41,42). On the other hand, both Trp-6 and Trp-22 are near the active site. The indole ring of the latter is in Van der Waal's contact with the carboxamide ring of NADPH in the crystalline binary DHFR-NADPH and the ternary DHFR-MTX-NADPH complexes whereas the backbone atoms of Trp-6 are near the pyrimidine ring of MTX but the side chain points away from the active site. The relative paramagnetic broadening evident from the spectra in Figure 9,  $< 12$  Hz for Trp-6 and  $> 25$  Hz for Trp-22, is consistent with this general structure for solutions of the enzyme as well.

#### CONCLUDING REMARKS

This brief and highly selective survey presents an optimistic outlook for the utility of stable isotope labeling in the study of architecture and dynamics of biological systems by NMR spectroscopy. It is appropriate at this juncture, however, to emphasize some of the limitations of the method. As Matthews points out, and our discussion of DHFR illustrates, the most useful insights at this point in time will be obtained from the method when it is used to study systems whose crystal structures are known. In part, this derives from our inadequate understanding of the origin of  $^{13}\text{C}$  (and  $^{15}\text{N}$ ) shifts in macromolecules and macromolecular assemblages. This point is illustrated well by our other studies of [ $^{13}\text{C}$ -methyl]methionine labeled DHFR (35).

In Figure 10 are summarized the  $^{13}\text{C}$  NMR spectra in the S-methyl region for [ $^{13}\text{C}$ -Me]methionine enriched DHFR in the presence of a variety of substrates and effector analogs. There are seven methionine residues in DHFR from Streptococcus faecium and at least six S-methyl  $^{13}\text{C}$  resonances can be resolved in several of the spectra (36). The urea denatured enzyme exhibits a single resonance at 15.32 ppm. For the complete set of analogs studied, the S-methyl resonances of DHFR span a chemical shift range of 3.4 ppm. It has been suggested (44) that it is protein folding which immobilizes amino acid residues and that in turn gives rise to large  $^{13}\text{C}$  chemical shift dispersions in proteins.

Because a proton bearing  $^{13}\text{C}$  in an immobilized residue should exhibit a resonance which is extensively broadened by dipolar interactions, it has also been suggested that structural perturbations in proteins are best monitored in  $^{13}\text{C}$  NMR through a study of "non-protonated" quaternary carbons which should exhibit narrower lines and a higher degree of resolution. Although this is certainly true of the  $^{13}\text{C}_\gamma$  in the tryptophan residues of DHFR just described, the [ $^{13}\text{C}$ -Me]methionine residues of the same enzyme provide a remarkable exception to the generalization: not only are the  $^{13}\text{CH}_3$ -S shifts large but the lines are narrow.

London (45) has provided a theoretical explanation for this "exception" which may be encountered more frequently in macromolecules than previous theoretical treatments would suggest. The model he has developed is illustrated in Figure 11. It allows unrestricted rapid diffusion ( $D_2$ ) about the S- $\text{CH}_3$  bond coupled to restricted amplitude diffusion ( $\pm \theta = 90 - 180^\circ$ ) about the  $\text{CH}_2$ -S bond. The model is physically reasonable since the rotation of the methyl group does not require the creation of free volume and therefore should not be restricted by inter-residue interactions. Rotation about the  $\text{CH}_2$ -S bond, however, does require sweeping additional free volume and, therefore, should be restricted by inter-residue contacts. The combination of the two motions coupled to rotational diffusion of the protein as a whole imparts rapid pseudo-isotropic motion to the  $^{13}\text{C}$  methyl group with attendant narrow lines. Yet this model is not inconsistent with a partial immobilization of the methionyl side chains by the inter-residue contacts which cause the chemical shift dispersion. In this context, two things should be noted:

- (1) The  $^{13}\text{CH}_3$ -S linewidths, Nuclear Overhauser Enhancements, and  $T_1$  values could not be fit using a free internal diffusion model (45), that is to say the treatment is not a "grasping" force fit of the data; and
- (2) There is a semi-quantitative correlation (Table 1) between the restriction of the amplitude of diffusion about the  $\text{CH}_2$ -S bond (short  $T_1$  values) and the inter-residue induced chemical shifts from the (urea induced) 15.32 ppm "random coil" configuration of the protein.

As gratifying as this exercise is in resolving an apparent conflict between our intuitions about what induces chemical shifts and restricted motions in macromolecules, we are still left in a quandary about the origin of the  $^{13}\text{C}$  chemical shifts not only of the methionyl residues but also of the Trp residues of DHFR. There is a missing data base that may not be provided even in the study of environmental and structural perturbations of amino acids and peptides -- it simply may not be possible to artificially construct those shift perturbations that enzymes and proteins supply so naturally. This underlines the need at this point in time to fold the results of x-ray crystallography

TABLE 1. CHEMICAL SHIFTS AND RELAXATION TIMES OF THE  $^{13}\text{CH}_3$  RESONANCES IN  $[\text{}^{13}\text{C-Me}]$ METHIONINE ENRICHED DHFR COMPLEXES.

<u>Complex</u>	<u>Resonance Shift (ppm)</u>	<u><math>\text{NT}_1</math> Value (msec)</u>
Enzyme Alone	15.35	590
	14.99	470
	14.66	500
Enzyme - MTX	15.37	720
	15.24	400
	14.95	410
	14.74	330
	14.57	460
	14.18	370
	15.36	710
Enzyme - MTX - NADP	15.24	560
	15.03	470
	14.68	350
	14.44	480
	13.96	420

into the design of NMR experiments on isotopically labeled macromolecules and macromolecular assemblages. Consistent with the main theme of this conference, I would also point out that isotope labeling in conjunction with the use of properly designed shift and relaxation reagents can carry us far in mapping enzyme-ligand interactions. We have briefly discussed this latter point in the outline of the [ $^{13}\text{C}_\gamma$ ]Trp labeled DHFR experiments and have conducted much more extensive studies of the interaction of labeled analogs with [ $^{13}\text{C}$ -Me]methionine enriched DHFR but time does not permit a discussion of the results.

\* This work performed under the auspices of the U. S. Department of Energy.

- (1) Dickerson, R. E.: 1972, *Ann. Rev. Biochem.* 41, pp. 815-842.
- (2) Perutz, M.: 1978, *Scientific American* 239, pp. 92-125.
- (3) Blow, D. M.: 1976, *Accounts Chemical Research* 9, pp. 145-152.
- (4) Kraut, J.: 1977, *Ann. Rev. Biochem.* 46, pp. 331-358.
- (5) Bachovchin, W. W. and Roberts, J. D.: 1978, *J. Am. Chem. Soc.* 100, pp. 8041-8047.
- (6) However, it appears that a determination of the root mean square displacements of the atoms may provide a method for mapping the dynamic features of a macromolecule (7,8).
- (7) Phillips, D. C. and Sternberg, M.: 1979, *J. Molec. Biol.* in press.
- (8) Frauenfelder, H., Petsko, G. A., and Tsernoglou, D.: 1979, *Nature*, submitted.
- (9) Matwiyoff, N. A. and Needham, T. E.: 1972, *Biochem. Biophys. Res. Commun.* 49, pp. 1158-1163.
- (10) Rossi-Bernardi, L. and Roughton, F. J.: 1967, *J. Physiol.* 189, p. 1.
- (11) Kilmartin, J. V. and Rossi-Bernardi, L.: "CO<sub>2</sub>: Chemical, Biological, and Physiological Aspects", Foster, R. E., Edsall, J. T., Otis, H. B., and Roughton, F. J. W., eds., Symposium at Haverford College, Haverford, PA, NASA SP-188, Library of Congress Catalog No. 77600831.
- (12) Roughton, F. J. W.: 1970, *Biochem. J.*, 117, p. 801.
- (13) Kilmartin, J. V. and Rossi-Bernardi, L.: 1969, *Nature*, 222, p. 1243.
- (14) Kilmartin, J. V. and Rossi-Bernardi, L.: 1971 *Biochem. J.* 124, p. 31.
- (15) Kilmartin, J. V., Fogg, J., Luzzana, M., and Rossi-Bernardi, L.: 1973, *J. Biol. Chem.* 248, p. 7039.
- (16) Arnone, A.: 1974, *Nature*, 247, pp. 143-145.
- (17) Matthew, J. B., Morrow, J. S., Wittebort, R. J., and Gurd, F. R. N.: 1977, *J. Biol. Chem.* 252, pp. 2234-2244, and references therein.
- (18) Wittebort, R. J., Hayes, D. F., Rothgeb, T. M., and Gurd, R. S.: 1978, *Biophys. J.* 24, pp. 765-778.
- (19) Silverman and co-workers (20), on the basis of the measurement of CO<sub>2</sub> kinetics in red cell suspensions by <sup>18</sup>O exchange, suggest that the intrinsic activity of carbonic anhydrase is the same in the cell and in homogeneous aqueous solution; but that the rate of access of CO<sub>2</sub> to carbonic anhydrase in intact red cells is slower than the catalytic hydration rate.
- (20) Tu, C., Wynns, G. C., McMurray, R. G., and Silverman, D. N.: 1978, *J. Biol. Chem.*, 253, p. 8178.
- (21) London, R. E., Gregg, C. T., and Matwiyoff, N. A.: 1975, *Science* 188, pp. 266-268.
- (22) London, R. E., Hildebrand, C. E., Olson, E. S., and

- Matwiyoff, N. A.: 1976, *Biochem.* 15, pp. 5480-5486.
- (23) See, for example: "The Molecular Basis of Membrane Function", Tosteson, D. C.: Editor, Prentice-Hall, Inc., New Jersey, 1969; Chapman, D.: 1975, *Biomembranes*, 7, p.1, and references therein.
  - (24) Bocian, D. F. and Chan, S. I.: 1978, *Ann. Rev. Phys. Chem.*, 29, p. 307.
  - (25) London, R. E., Walker, T. E., Matwiyoff, N. A., and Wilson, D. M.: 1979, *Chem. Phys. Lipids*, in press.
  - (26) Govil, G. and Smith, I. C. P.: 1973, *Biopolymers* 12, p. 2589.
  - (27) O'Connor, J., Nunez, H., and Barker, R.: 1979, *Biochem.* in press.
  - (28) Browne, D. T., Kenyon, G. L., Packer, E. L., Sternlicht, H., and Wilson, D. M.: 1973, *J. Am. Chem. Soc.* 95, p. 1316.
  - (29) Browne, D. T., Kenyon, G. L., Packer, E. L., and Wilson, D. M.: 1973, *Biochem. Biophys. Res. Commun.* 50, p. 42.
  - (30) Hunkapiller, M. W., Smallcombe, S. H., Whitaker, D. R., and Richards, J. H.: 1973, *J. Biol. Chem.* 248, p. 8306; *ibid*: 1973, *Biochem.* 12, p. 4732.
  - (31) Hunkapiller, M. W., Smallcombe, S. H., and Richards, J. H.: 1975, *Org. Mag. Res.* 7, p. 262.
  - (32) Browne, D. T., Earl, E. M., and Otvos, J. D.: 1976, *Biochem. Biophys. Res. Commun.* 72, p. 398.
  - (33) Chaiken, I. M., Cohen, J. S., and Sokolski, E. A.: 1974, *J. Am. Chem. Soc.* 96, p. 4703.
  - (34) Eakln, R. T., Morgan, L. O., and Matwiyoff, N. A.: 1975, *Biochem. J.* 152, p. 529.
  - (35) Cocco, L., Blakley, R. L., Walker, T. E., London, R. E., and Matwiyoff, N. A.: 1977, *Biochem. Biophys. Res. Commun.* 76, p. 183.
  - (36) Blakley, R. L., Cocco, L., London, R. E., Walker, T. E., and Matwiyoff, N. A.: 1978, *Biochem.* 17, p. 2284.
  - (37) London, R. E., Groff, J. P., and Blakley, R. L.: 1979, *Biochem. Biophys. Res. Commun.* 86, p. 779.
  - (38) London, R. E., Groff, J. P., and Blakley, R. L.: work in progress.
  - (39) Gleisner, J. M., Peterson, D. L., and Blakley, R. L.: 1974, *Proc. Nat. Acad. Sci.* 71, p. 3001.
  - (40) Matthews, D. A., Alden, R. A., Freer, S. T., Xuong, N., and Kraut, J.: 1979, *J. Biol. Chem.*, in press.
  - (41) Matthews, D. A., Alden, R. A., Bolin, J. T., Freer, S. T., Hamlin, R., Xuong, N., Kraut, J., Poe, M., Williams, M., and Hoogsteen, K.: 1977, *Science* 197, p. 452.
  - (42) Matthews, D. A.: 1979, *Biochem.* 18, p. 1602.
  - (43) Cocco, L., Blakley, R. L., and London, R. E.: work in progress.
  - (44) Oldfield, E., Norton, R. S., and Allerhand, A.: 1975, *J. Biol. Chem.* 250, p. 6368.
  - (45) London, R. E. and Avitable, J.: 1978, *J. Am. Chem. Soc.* 100, p. 7159.



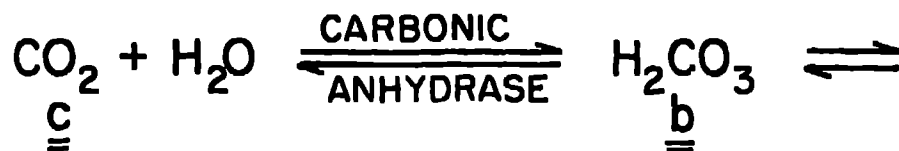
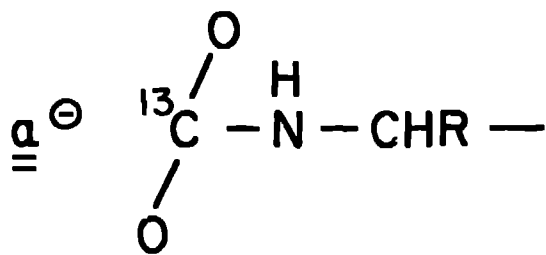
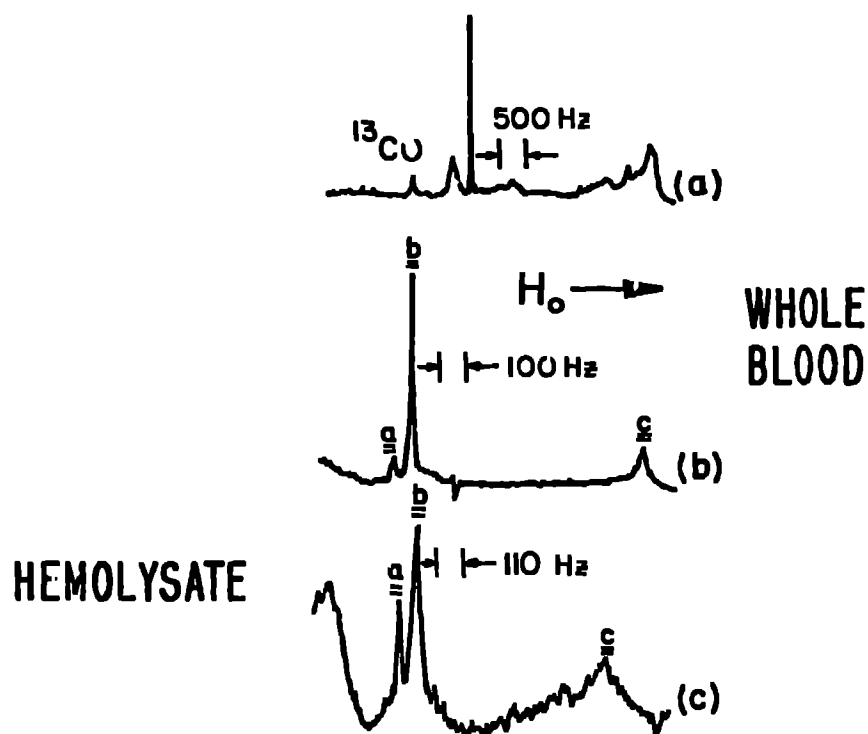


Figure 1. Proton noise decoupled  $^{13}\text{C}$  NMR spectra: (a) Dog whole blood +  $^{13}\text{CO}$ , 65,000 pulses; (b) Human whole blood +  $^{13}\text{CO}_2$ , 14,000 pulses; (c) Human whole blood +  $^{13}\text{CO}_2$  + carbonic anhydrase, 12,000 pulses. Signals a, b, and c are assigned to the hemoglobin carhamino complexes, carbonic acid, and  $\text{CO}$ , respectively.

# LIPIDS IN VESICLES (DISPERSED IN D<sub>2</sub>O)

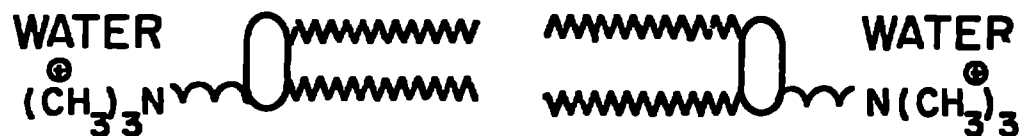
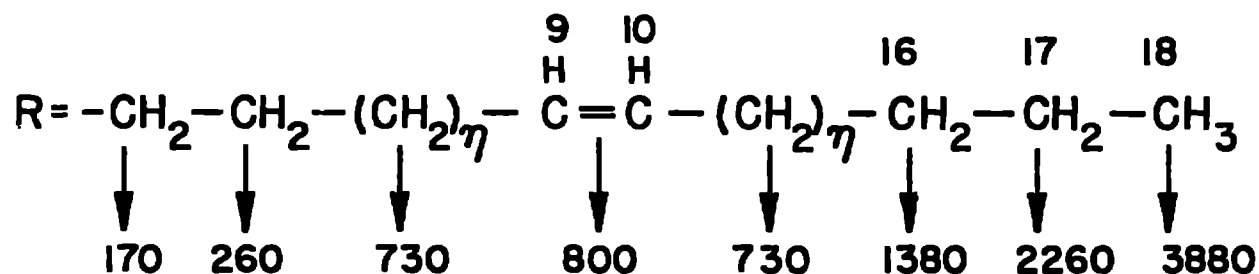
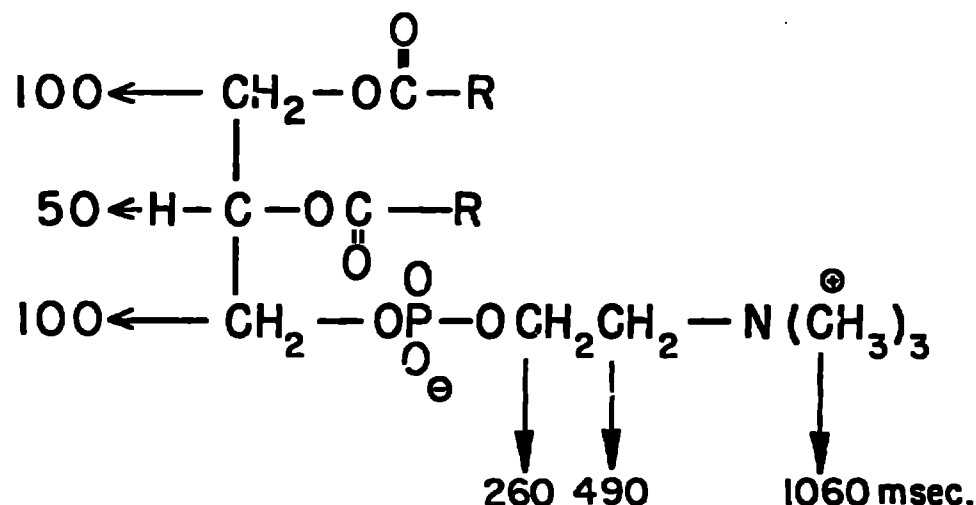


Figure 2. Spin lattice relaxation times ( $T_1$ ) in msec for the carbon atoms in lecithin vesicles. The  $T_1$  values observed are consistent with a high degree of mobility or fluidity of the lipid bilayer. The vesicles are a micelle structure with the polar head groups exposed to water and the lipid chains packed together in a hydrophobic environment

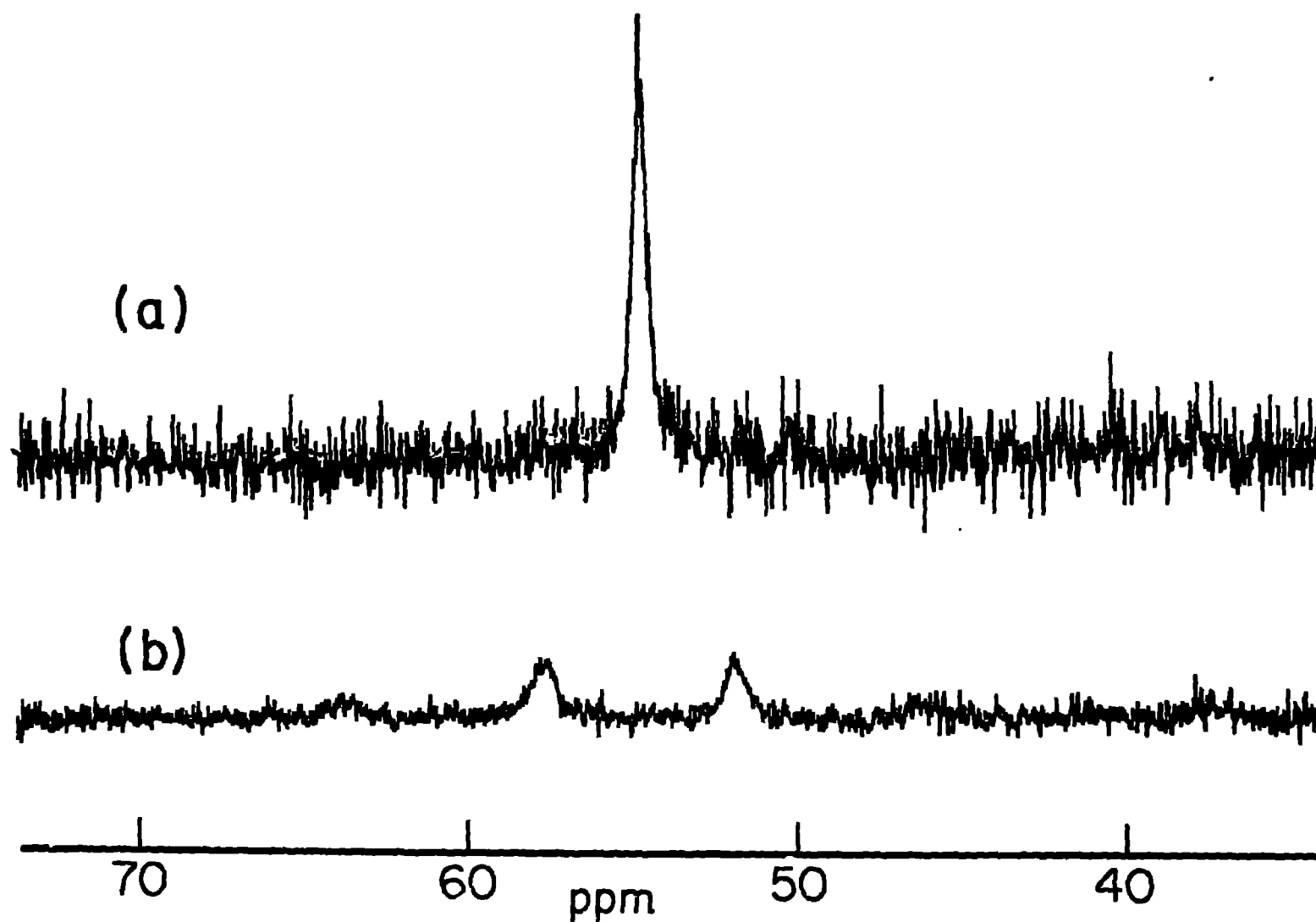


Figure 3. Proton decoupled (a) and coupled (b)  $^{13}\text{C}$  FT NMR spectra of the choline resonance of sonicated vesicles prepared from extracted CHO cell lipids. Spectrum a represents 8200 pulses and spectrum b 100 850. Sample temperature was 11°C and a 2-s delay between pulses was used for the accumulation time.

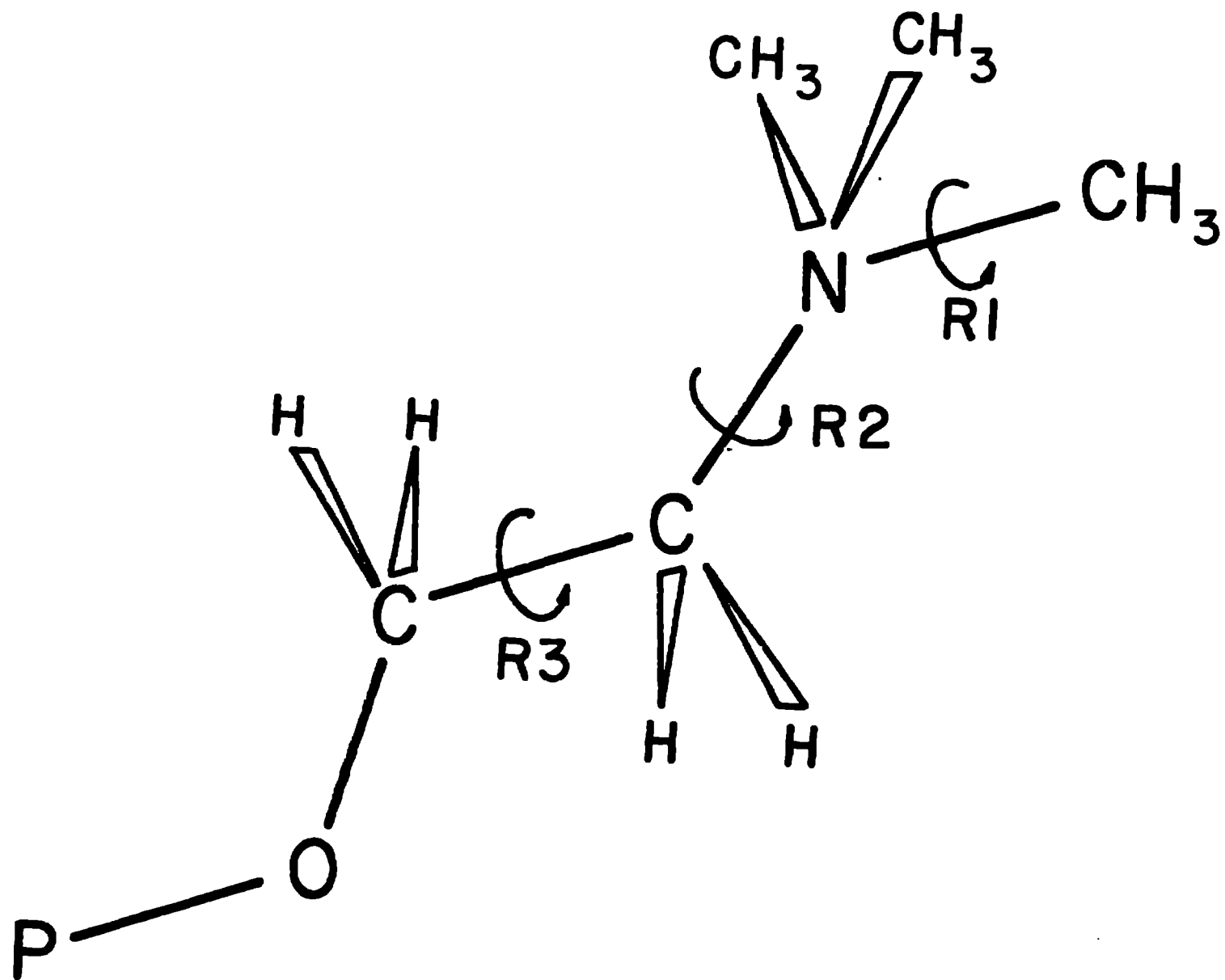


Figure 4. Illustration of the possible motions contributing to the relaxation of the choline methyl groups.

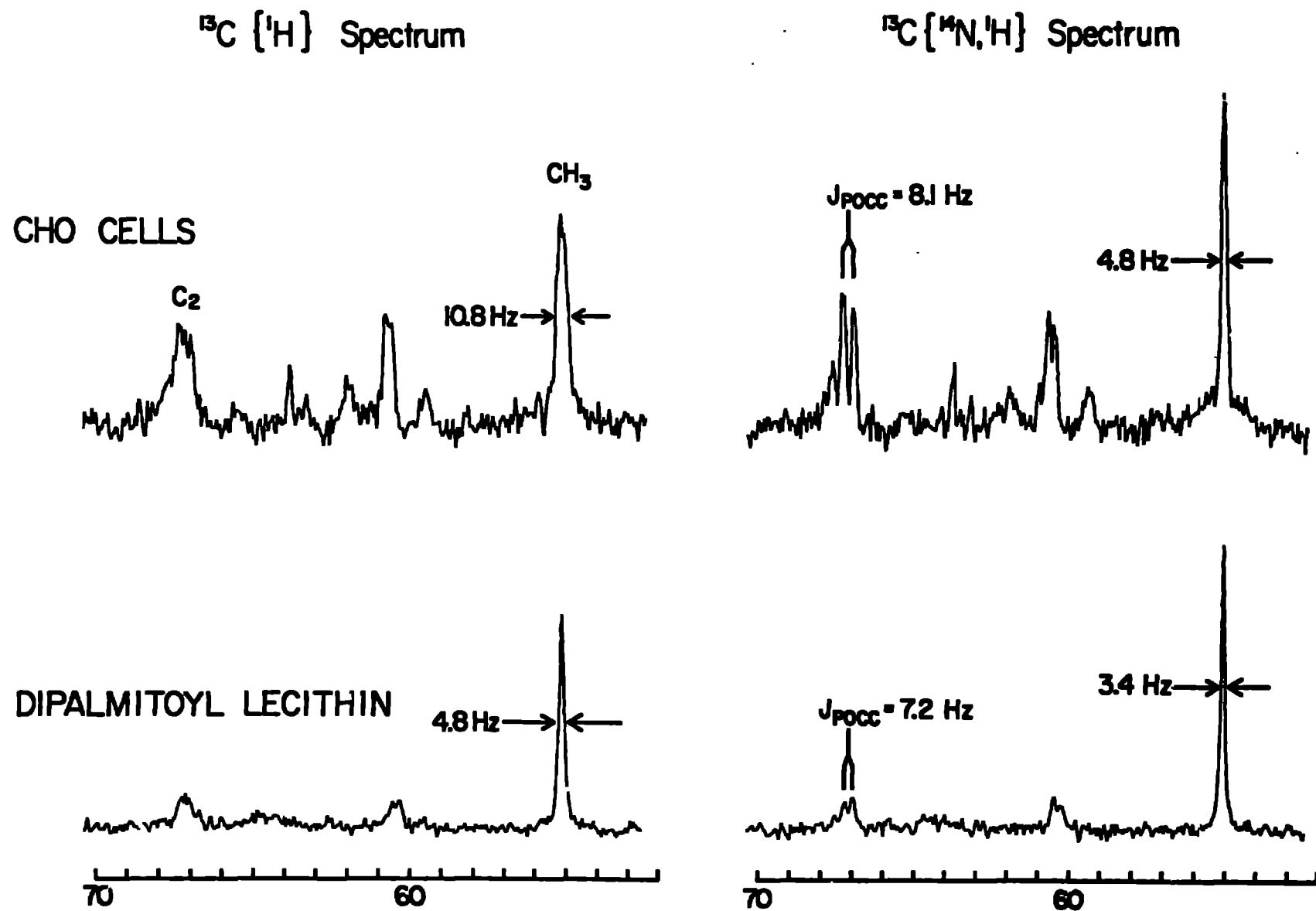


Figure 5.  $^{13}\text{C} \{^1\text{H}\}$  and  $^{13}\text{C} \{^{14}\text{N}, ^1\text{H}\}$  spectra (52-70 ppm) of sonicated dipalmitoyl lecithin vesicles in  $\text{H}_2\text{O}$  (50°C) (lower) and Chinese Hamster Ovary (CHO) cells (upper) grown on an F-10 medium supplemented with calf serum and 14 mg/l of  $^{13}\text{C}$  enriched choline. Spectra of the CHO cells were obtained in  $\text{H}_2\text{O}$  at 20°C and represent an 18 hr.

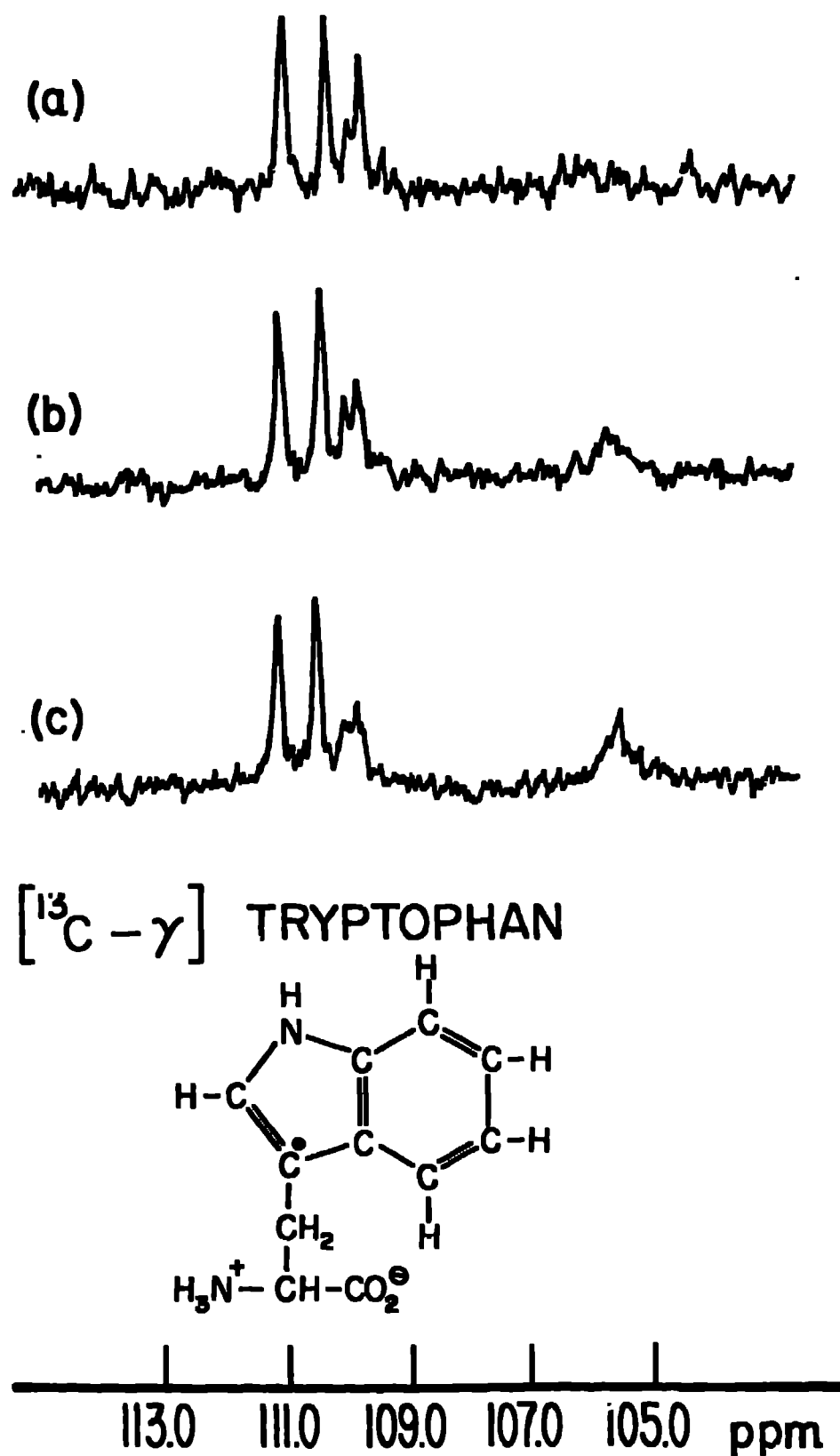


Figure 6.  $^{13}\text{C}$  NMR spectra of  $[\gamma\text{-}^{13}\text{C}]$ tryptophan labeled dihydrofolate reductase at various temperatures.

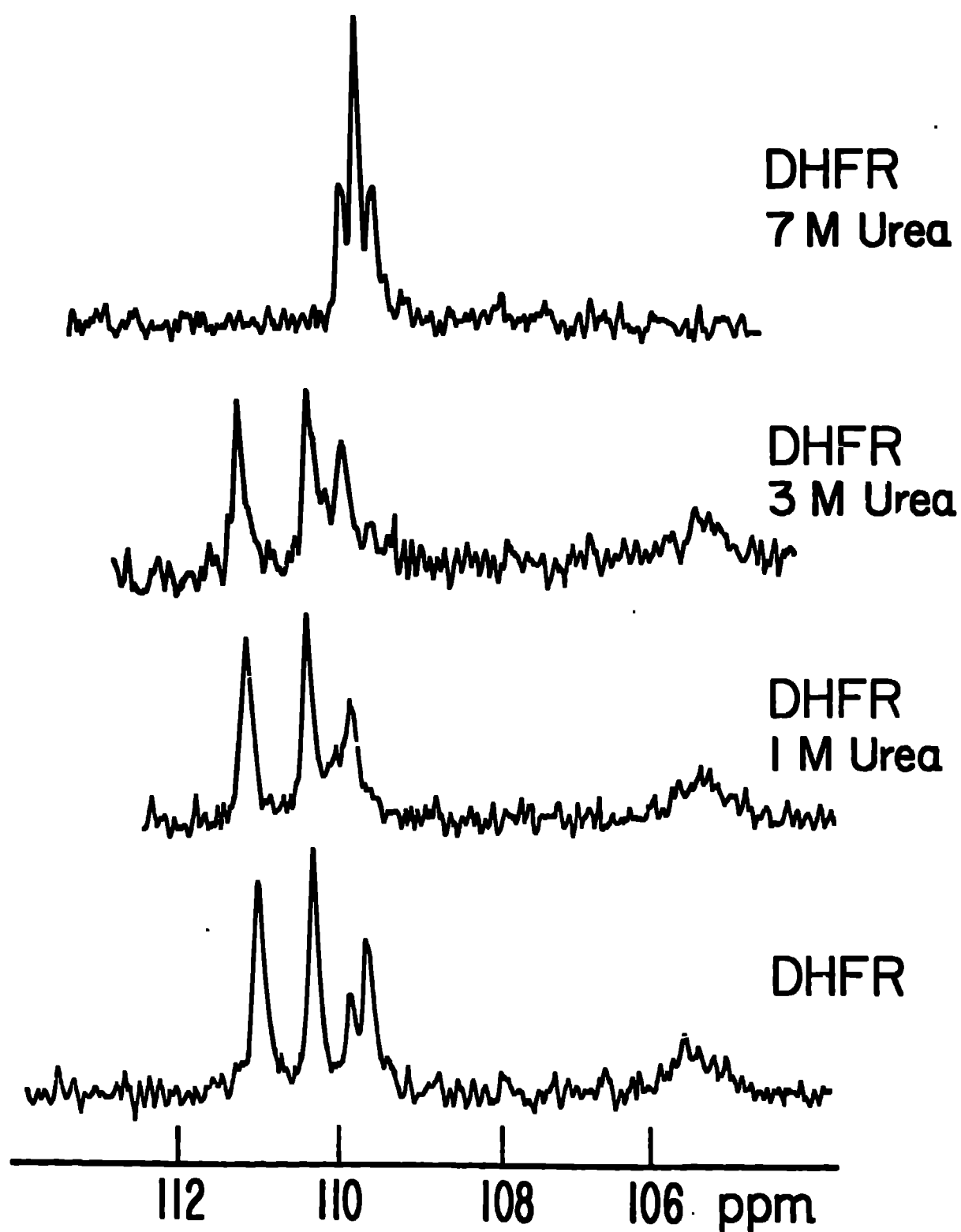


Figure 7.  $^{13}\text{C}$  NMR spectra of  $[\gamma\text{-}^{13}\text{C}]$ tryptophan labeled dihydrofolate reductase (15°C) in various stages of denaturation with urea. Urea concentrations are as indicated on each spectrum

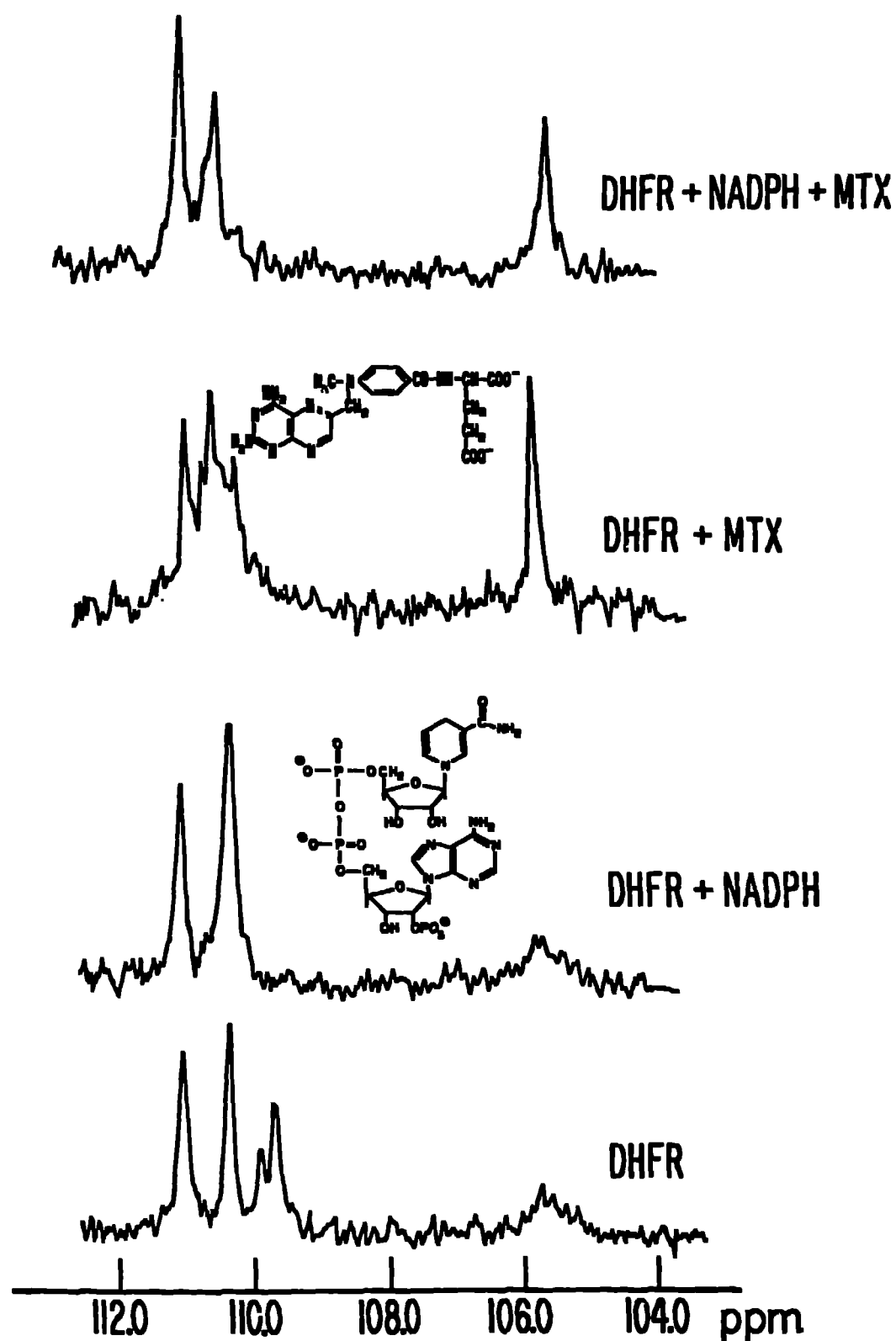


Figure 8.  $^{13}\text{C}$  NMR spectra of a series of binary and ternary complexes of dihydrofolate reductase (15°C) labeled with  $[\gamma\text{-}^{13}\text{C}]$ tryptophan. From bottom to top the complexes are as follows: uncomplexed enzyme, enzyme-NADPH binary, enzyme-methotrexate binary,





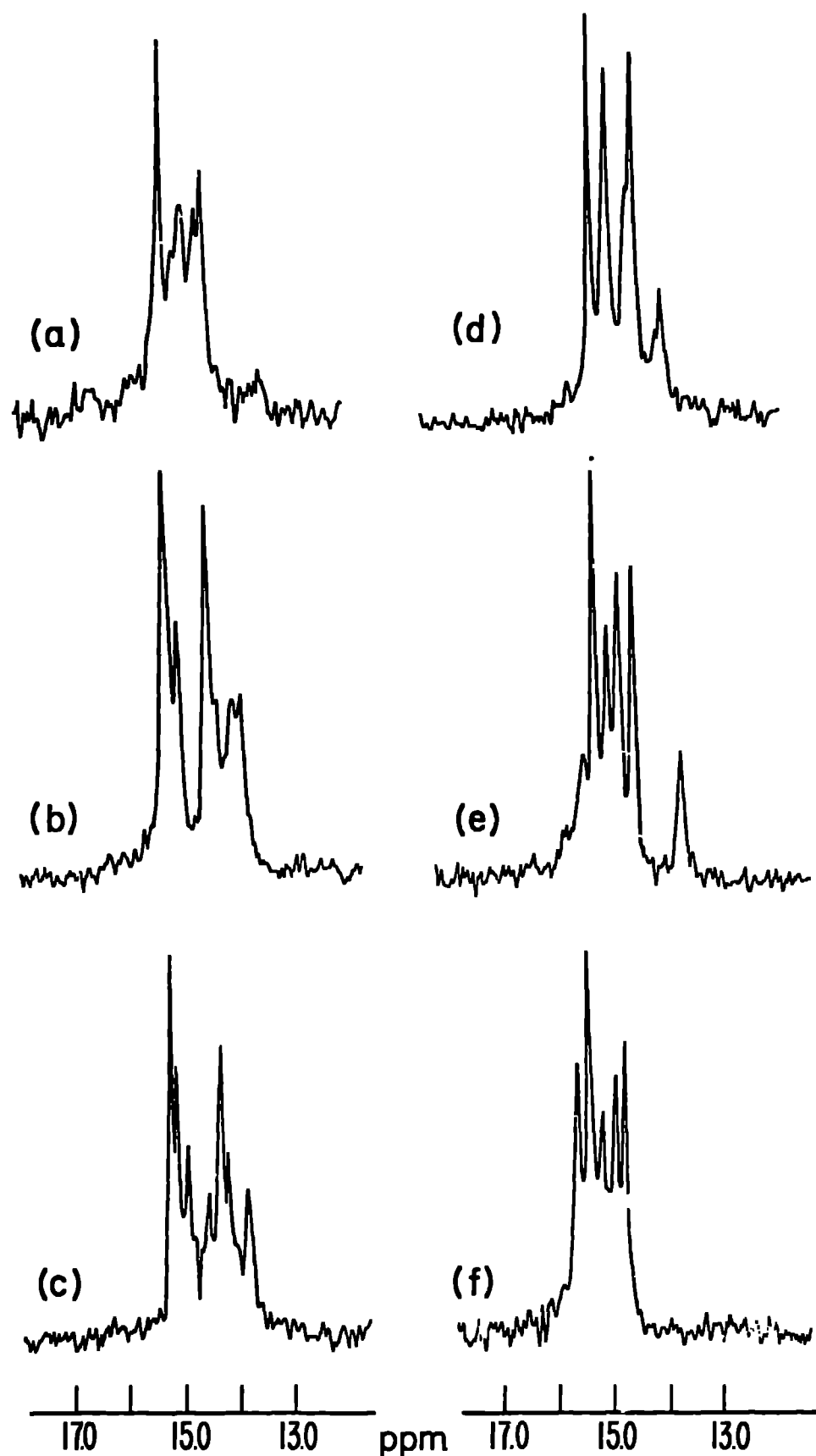


Figure 10.  $^{13}\text{C}$  NMR spectra of ternary complexes of dihydrofolate reductase labeled with [methyl- $^{13}\text{C}$ ]methionine. (a) Enzyme-dihydrofolate- $\text{NADP}^+$ ,  $15^\circ\text{C}$ ; (b) Enzyme-methotrexate- $\text{NADP}^+$ ,  $25^\circ\text{C}$ ; (c) Enzyme-methotrexate- $\text{NADPH}$ ,  $25^\circ\text{C}$ ; (d) Enzyme-methotrexate- $\text{PADPR}$ ,  $25^\circ\text{C}$ ; (e) Enzyme-diaminopyrimidine- $\text{NADPH}$ ,  $20^\circ\text{C}$ ; (f) Enzyme-dichloromethotrexate- $\text{NADPH}$ ,  $25^\circ\text{C}$ .

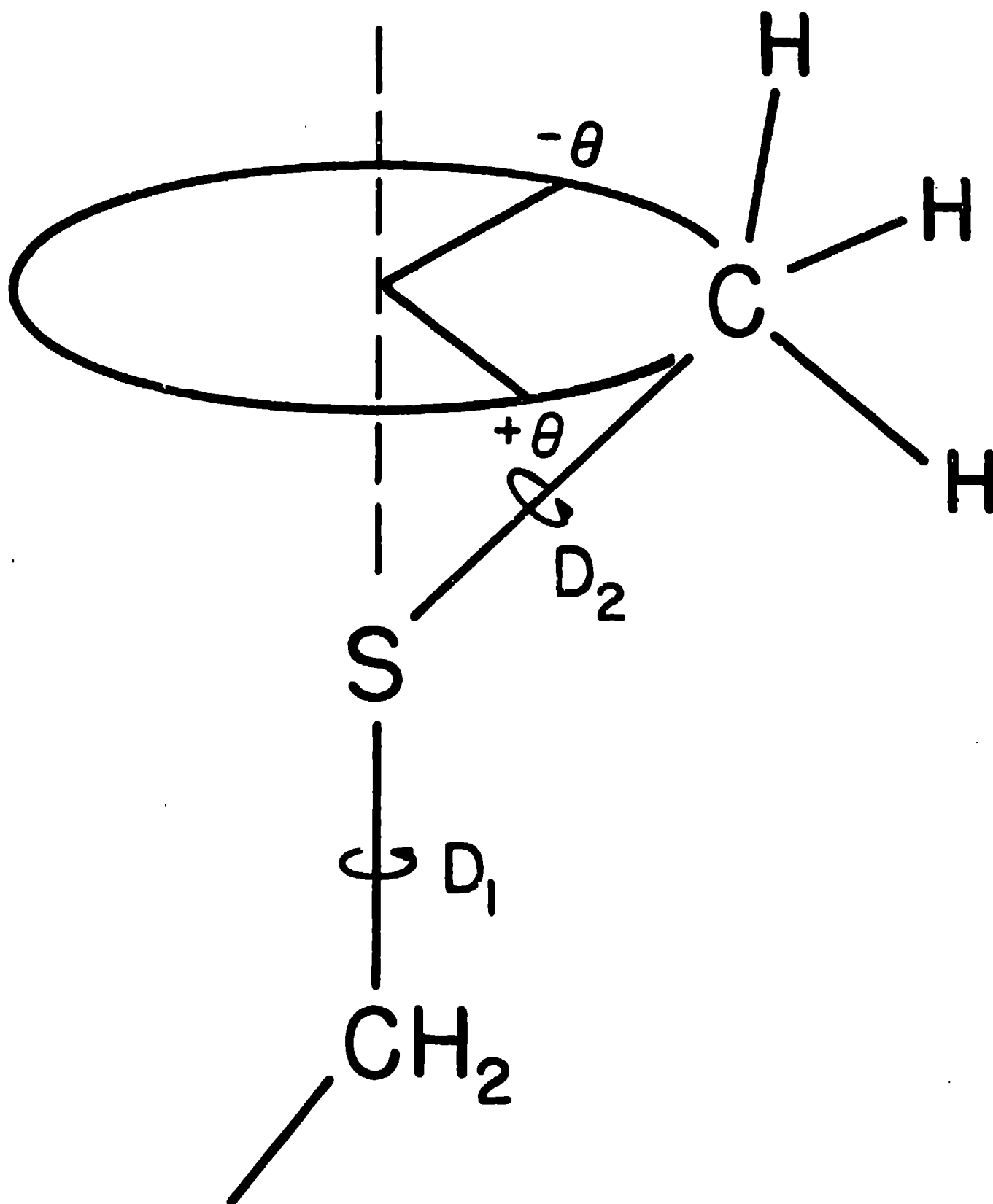


Figure 11. Illustration of the possible motions around the sulfur atom in methionine. The combination of motions about  $\text{D}_1$  (restricted) and  $\text{D}_2$  (unrestricted) leads to relatively narrow lines for the methyl  $^{13}\text{C}$  resonance in protein methionyl side chains of dihydrofolate reductase.